Analytical validity of nanopore sequencing for rapid SARS-CoV-2 genome analysis

Rowena A. Bull[1,2]*, Thiruni Adikari[1,2]*, Jillian M. Hammond[3], Igor Stevanovski[3], James M. Ferguson[3], Alicia G. Beukers[4], Zin Naing[2,5], Malinna Yeang[2,5], Andrey Verich[1], Hasindu Gamaarachichi[3,6], Ki Wook Kim[2,5], Fabio Luciani[1,2], Sacha Stelzer-Braid[2,5], John-Sebastian Eden[7,8], William D. Rawlinson[2,5,9,10], Sebastiaan J. van Hal[4,11] & Ira W. Deveson[3,12#]

* These authors contributed equally.
# Correspondence: i.deveson@garvan.org.au

[1] The Kirby Institute for Infection and Immunity, University of New South Wales, Sydney, NSW, Australia.

[2] School of Medical Sciences, Faculty of Medicine, University of New South Wales, Sydney, NSW, Australia.

[3] Kinghorn Centre for Clinical Genomics, Garvan Institute of Medical Research, Sydney, NSW, Australia.

[4] NSW Health Pathology, Department of Infectious Diseases and Microbiology, Royal Prince Alfred Hospital, Sydney, NSW, Australia.

[5] Virology Research Laboratory, Serology and Virology Division (SAViD), NSW Health Pathology, Prince of Wales Hospital, Sydney, NSW, Australia.

[6] School of Computer Science and Engineering, University of New South Wales, Sydney, NSW, Australia.

[7] Marie Bashir Institute for Infectious Diseases and Biosecurity & Sydney Medical School, The University of Sydney, Sydney, NSW, Australia

[8] Centre for Virus Research, Westmead Institute for Medical Research, Sydney, NSW, Australia

[9] School of Women's and Children's Health, Faculty of Medicine, University of New South Wales, Sydney, NSW, Australia.

[10] School of Biotechnology and Biomolecular Sciences, Faculty of Science, University of New South Wales, Sydney, NSW, Australia.

[11] Central Clinical School, University of Sydney, Sydney, NSW, Australia.

[12] St Vincent's Clinical School, Faculty of Medicine, University of New South Wales, Sydney, NSW, Australia.

ABSTRACT

Viral whole-genome sequencing (WGS) provides critical insight into the transmission and evolution of Severe Acute Respiratory Syndrome Coronavirus 2 (SARS-CoV-2). Long-read sequencing devices from Oxford Nanopore Technologies (ONT) promise significant improvements in turnaround time, portability and cost, compared to established short-read sequencing platforms for viral WGS (e.g., Illumina). However, adoption of ONT sequencing for SARS-CoV-2 surveillance has been limited due to common concerns around sequencing accuracy. To address this, we performed viral WGS with ONT and Illumina platforms on 157 matched SARS-CoV-2-positive patient specimens and synthetic RNA controls, enabling rigorous evaluation of analytical performance. Despite the elevated error rates observed in ONT sequencing reads, highly accurate consensus-level sequence determination was achieved, with single nucleotide variants (SNVs) detected at >99% sensitivity and >98% precision above a minimum ~60-fold coverage depth, thereby ensuring suitability for SARS-CoV-2 genome analysis. ONT sequencing also identified a surprising diversity of structural variation within SARS-CoV-2 specimens that were supported by evidence from short-read sequencing on matched samples. However, ONT sequencing failed to accurately detect short indels and variants at low read-count frequencies. This systematic evaluation of analytical performance for SARS-CoV-2 WGS will facilitate widespread adoption of ONT sequencing within local, national and international COVID-19 public health initiatives.

INTRODUCTION

Severe **A**cute **R**espiratory **S**yndrome **Co**rona**v**irus **2** (SARS-CoV-2) is the causative pathogen for COVID-19 disease[1,2]. SARS-CoV-2 is a positive-sense single-stranded RNA virus with a ~30 kb poly-adenylated genome[1,2]. Complete genome sequences published in January 2020[1,3] enabled development of RT-PCR assays for SARS-CoV-2 detection that have served as the diagnostic standard during the ongoing COVID-19 pandemic[4].

Whole-genome sequencing (WGS) of SARS-CoV-2 provides additional data to complement routine diagnostic testing. Viral WGS informs public health responses by defining the phylogenetic structure of disease outbreaks[5]. Integration with epidemiological data identifies transmission networks and can infer the origin of unknown cases[6-12]. Largescale, longitudinal surveillance by viral WGS may also provide insights into virus evolution, with important implications for vaccine development[13-15].

WGS can be performed via PCR amplification or hybrid-capture of the reverse-transcribed SARS-CoV-2 genome sequence, followed by high-throughput sequencing. Short-read sequencing technologies (e.g., Illumina) enable accurate sequence determination and are the current standard for pathogen genomics. However, long-read sequencing devices from Oxford Nanopore Technologies (ONT) offer an alternative with several advantages. ONT devices are portable, cheap, require minimal supporting laboratory infrastructure or technical expertise for sample preparation, and can be used to perform rapid sequencing analysis with flexible scalability[16].

The use of ONT devices for viral surveillance has been demonstrated during Ebola, Zika and other disease outbreaks[17-19]. Although protocols for ONT sequencing of SARS-CoV-2 have been established, adoption of the technology has been limited by concerns around its accuracy. ONT devices exhibit lower read-level sequencing accuracy than short-read platforms[20-22]. This may have a disproportionate impact on SARS-CoV-2 analysis, due to the virus' low mutation rate (8×10^{-4} substitutions per site per year[23]), which ensures erroneous (false-positive) or undetected (false-negative) genetic variants have a strong confounding effect.

In order to address concerns regarding ONT sequencing accuracy and evaluate its analytical validity for SARS-CoV-2 genomics, we have performed amplicon-based nanopore and short-read WGS on matched SARS-CoV-2-positive patient specimens and synthetic RNA controls, allowing rigorous evaluation of ONT performance characteristics.

RESULTS

Analysis of synthetic SARS-CoV-2 controls

Synthetic DNA or RNA reference standards can be used to assess the accuracy and reproducibility of next-generation sequencing assays[24]. We first sequenced synthetic RNA controls that were generated by *in vitro* transcription of the SARS-CoV-2 genome sequence. The controls matched the Wuhan-Hu-1 reference strain at all positions, allowing analytical errors to be unambiguously identified. To mimic a real-world viral WGS experiment, synthetic RNA was reverse-transcribed then amplified using multiplexed PCR of 98 × ~400 bp amplicons that enabled evaluation of ~95% of the SARS-CoV-2 genome. Eight independent replicates were sequenced on ONT PromethION and Illumina MiSeq instruments (see **Methods**).

We aligned the resulting reads to the Wuhan-Hu-1 reference genome to assess sequencing accuracy and related quality metrics (**Fig. S1a-i**). Illumina and ONT platforms exhibited distinct read-level error profiles, with the latter characterised by an elevated rate of both substitution (23-fold) and insertion-deletion (indel) errors (76-fold; **Table 1**; **Fig. S1d,e**). Per-base error frequency profiles showed clear correlation between ONT replicates (substitution $R^2 = 0.67$; indel $R^2 = 0.82$; **Fig. S1f,g**). This indicates that ONT sequencing errors are not entirely random but are influenced by local sequence context. For example, indel errors were enriched (1.4-fold) at low-complexity sequences within the SARS-CoV-2 genome (i.e., sites with homopolymeric or repetitive content; ~1% of the genome; **Fig. S1d**). Illumina error profiles showed weaker correlation between replicates (substitution $R^2 = 0.15$; indel $R^2 = 0.42$), indicating that short-read sequencing errors were less systematic than for ONT libraries (**Fig. S1h,i**).

Despite their distinct error profiles, both sequencing platforms demonstrated high consensus-level sequencing accuracy across the SARS-CoV-2 genome. We used *iVar* and *Medaka* to determine consensus

genome sequences for Illumina and ONT libraries, respectively (see **Methods**). We detected just two erroneous variant candidates in a single ONT library (**Table 1**). Both of these were single-base insertions occurring at low-complexity sites (**Fig. S2**), with no erroneous SNVs detected in any replicate (n = 8). All Illumina libraries exhibited perfect accuracy (**Table 1**). Therefore, the sequencing artefacts affecting both technologies had minimal impact on the accuracy of consensus-level sequence determination, with indel errors in ONT samples being a possible exception.

Analysis of matched patient isolates

To further evaluate the suitability of ONT sequencing for SARS-CoV-2 genomics, we conducted rigorous proficiency testing using *bona fide* clinical specimens. We performed ONT and Illumina WGS on matched, de-identified SARS-CoV-2-positive cases collected at public hospital laboratories in Eastern & Southern New South Wales and Metropolitan Sydney from March-May 2020 (see **Methods**; **Supplementary Table 1**). The SARS-CoV-2 genome was enriched by PCR amplification, using a custom set of 14 × ~2.5 kb amplicons[6] that covers 29783/29903 bp (99.6%) of the genome, including 100% of annotated protein-coding positions. Pooled amplicons then underwent parallel library preparation and sequencing on an ONT GridION/PromethION and an Illumina MiSeq instrument (see **Methods**). Short-read sequencing was performed according to a pathogen genomics accredited diagnostic workflow in a reference NSW Health Pathology laboratory, enabling direct comparison of nanopore sequencing to the established standard for pathogen genomics.

In total, we obtained complete (99.6%) genome coverage with both technologies for 157 matched positive cases (**Supplementary Table 1**). By comparison to the Wuhan-Hu-1 reference strain, Illumina sequencing identified 7.7 consensus single-nucleotide variants (SNVs) and 0.04 indels, on average, per sample. A further 1.0 SNVs and 0.2 indels per sample were detected at sub-consensus read-count frequencies (20 – 80%), indicative of intra-specimen genetic diversity (see below). Excluding positions with evidence of sub-consensus variation, this provides an overall comparison set of 1201 consensus variants and 4,674,554 positions that match the reference strain in a given sample, against which to assess the accuracy of SARS-CoV-2 nanopore sequencing (**Supplementary Table 1**).

We used *Medaka* to identify consensus SNVs and indels with ONT sequencing data (see **Methods**), detecting 7.9 SNVs and 1.2 indels, on average, per sample (**Supplementary Table 2**). In general, ONT SNV candidates were highly concordant with the Illumina comparison set. Illumina SNVs were detected with 99.50% sensitivity and 98.26% precision (**Table 2**). Erroneous candidates (false-positives) were more frequent than undetected SNVs (false-negatives), occurring in 15/157 (9%) and 5/157 (3%) samples, respectively (**Supplementary Table 2**). Overall, we found 97.78% concordance between ONT and Illumina SNVs, as measured by Jaccard similarity, with identical results in 139/157 samples (88%; **Table 2**). In contrast to SNVs, ONT sequencing failed to detect any of the seven consensus indels in the Illumina comparison set, with all candidate indels being classified as false-positives (**Table 2**; **Supplementary Table 2**). While the scarcity of consensus indels detected with either technology prevented a more thorough evaluation of indel accuracy, it appears that ONT sequencing is inadequate for accurate detection of small indels in the SARS-CoV-2 genome.

Evaluation of false-positive and false-negative variant candidates detected with ONT sequencing data showed that these disproportionately occurred in low-complexity sequences, which are known to be refractory to ONT base-calling algorithms[20]. For example, false-positive and/or false-negative SNVs were found within a 21 bp T-rich site in the *orf1ab* gene in multiple samples (**Fig. S3a,b**). We identified fifteen problematic low-complexity sites in the SARS-CoV-2 genome ranging in size from 9 to 42 bp in length that showed elevated read-level sequencing error rates (**Fig. S1d**; **Supplementary File 1**). Exclusion of these positions (~1% of the genome) improved the fidelity of ONT variant detection, with consensus SNVs in the Illumina comparison set being detected with 99.83% sensitivity and 99.15% precision. Overall Jaccard similarity increased to 98.98%, with identical results between ONT and Illumina data in 144/157 (92%) of samples (**Table 2**; **Supplementary Table 3**). This suggests the accuracy of nanopore WGS may be improved via the exclusion of a small number of 'blacklist' low-complexity sites in the SARS-CoV-2 genome from downstream analysis.

We next assessed the impact of sequencing depth on ONT performance. To do so, we down-sampled nanopore sequencing reads from a uniform 200-fold coverage across the SARS-CoV-2 genome and repeated variant detection across a range of coverage depths (see **Methods**). Relatively low coverage was required to detect SNVs with high sensitivity, with ≥99% sensitivity observed at ≥30-fold coverage depth and 151/157 (96%) samples showing perfect SNV sensitivity (**Fig. 1a**). However, an increase in false-positive rate was observed below ~60-fold coverage, resulting in an overall decline in SNV concordance at coverage increments below this (**Fig. 1b**). As above, excluding error-prone low-complexity sequences afforded consistent improvements to sensitivity and overall concordance across the range of depths tested (**Fig. 1a,b**). These results suggest that ≥60-fold coverage depth is required for accurate detection of consensus SNVs by nanopore sequencing, with minimal improvement observed above this level.

In summary, ONT sequencing enabled highly accurate detection of consensus-level SNVs in SARS-CoV-2 patient isolates but appears generally unsuitable for the detection of small indel variants.

Detection of intra-specimen variation

Within-host genetic diversity is a common feature of viral infections and resolving this diversity is informative for studies of pathogenesis, transmission and vaccine design[25,26]. Therefore, we next evaluated the capacity of nanopore sequencing to identify intra-specimen genetic variation by detecting variants present at sub-consensus frequencies (i.e. variants detected in <80% of mapped reads). Analysis of the SARS-CoV-2 synthetic RNA controls (see above) showed that sequencing artefacts in Illumina libraries could be misinterpreted as variants at read-count frequencies below ~20% (**Fig. S2b**), effectively establishing a lower bound for variant detection. We therefore limited our analysis to variants detected at ≥20% frequency, taking variants detected by Illumina sequencing above this level to be genuine. Overall, short-read sequencing identified sub-consensus variants (20-80%) in 54/157 samples, comprising 156 SNVs and 20 indels (**Supplementary Table 4**).

Using *Varscan2*, we identified 154 sub-consensus SNV candidates in ONT sequencing libraries (**Supplementary Table 4**). We detected 119 SNVs (sensitivity = 76.3%) in the Illumina comparison set and 25 false-positives (precision = 82.6%; **Supplementary Table 4**). Read-count frequencies for variants identified with both technologies were correlated (R^2 = 0.69), indicating that these were *bona fide* variants, rather than sequencing artefacts (**Fig. 1c**). While the overall performance of sub-consensus SNV detection was quite poor, most false-positives and false-negatives were confined to the lower end of the frequency range assessed here (**Fig. 1c,d**). For example, SNVs at high (60-80%) and intermediate (40-60%) sub-consensus frequencies were detected with relatively high sensitivity (95.7%, 91.3%) and precision (100%, 97.7%), whereas low-frequency variants (20-40%) were detected with low sensitivity (63.2%) and precision (69.6%; **Fig. 1d**). Unsurprisingly, the high rate of indel errors in ONT sequencing libraries meant that they were unsuitable for detecting indel diversity, with errors overwhelming true variants (**Supplementary Table 4**).

In summary, ONT sequencing enabled detection of within-specimen SNVs at frequencies from ~40-80% with adequate accuracy but was generally unsuitable for the detection of indels or rare SNVs (< 40%).

Detection of structural variation

Large genomic deletions or rearrangements can have a major impact on virus function and evolution, however, there are currently just a few reported cases of SARS-CoV-2 specimens harbouring structural variants (SVs)[27,28]. Therefore, we next evaluated the detection of SVs in SARS-CoV-2 specimens with ONT sequencing. We used *NGMLR* and *Sniffles* to identify potential SVs in ONT libraries and validated these with supporting evidence from short-read sequencing (see **Methods**).

Across all SARS-CoV-2 patient specimens, we detected sixteen candidate deletions ranging in size from 15-1,840 bp (**Table 3**), while no other SV types were identified. Of these, 13/16 were supported by split short-read alignments and/or discordant read-pairs in matched Illumina libraries (**Fig. S4a**; **Table 3**). For 7/16 candidates, short-read evidence confirmed the presence of the deletion but indicated that the breakpoint position was not accurately placed by ONT reads (**Fig. S4b**; **Table 3**). Among the thirteen deletions detected by both platforms were examples in genes *S*, *M*, *N*, *ORF3*, *ORF6*, *ORF8* and *orf1ab* (**Table 3**). Only one variant,

a 328 bp deletion in *ORF8* (**Fig. S4c**), was detected in multiple specimens, although highly similar (but not identical) 28 bp and 29 bp deletions were also detected in *S* in two unrelated specimens (**Fig. S4d**).

Overall, this analysis demonstrates that large deletions can be reliably detected using ONT sequencing and suggests that structural variation in the SARS-CoV-2 genome is more common and diverse than currently appreciated.

DISCUSSION

Viral WGS can be used to study the transmission and evolution of SARS-CoV-2, and is increasingly recognised as a critical tool for public health responses to COVID-19. Nanopore sequencing offers an alternative to established short-read platforms for viral WGS with several advantages. ONT devices: (*i*) are relatively inexpensive, highly portable and require minimal associated laboratory infrastructure; (*ii*) enable rapid generation of sequencing data and even real-time data analysis; (*iii*) require comparatively simple procedures for library preparation and; (*iv*) offer flexibility in sample throughput, accommodating single (e.g., Flongle), multiple (e.g., MinION/GridION) or tens/hundreds (e.g., PromethION) of specimens per flow-cell[16,18,29]. Therefore, ONT sequencing could further empower SARS-CoV-2 surveillance initiatives by enabling point-of-care WGS analysis and improved turnaround time for critical cases, particularly in isolated or poorly resourced settings.

Due to the relatively low mutation rate observed in SARS-CoV-2[23] , accurate sequence determination is vital to correctly define the phylogenetic structure of disease outbreaks. With ONT sequencing known to exhibit higher read-level sequencing error rates than short-read technologies[20-22], reasonable concerns exist about suitability of the technology for SARS-CoV-2 genomics. Moreover, public databases for SARS-CoV-2 data (e.g., GISAID: https://www.gisaid.org/) already contain consensus genome sequences generated via ONT sequencing, potentially confounding investigations that rely on these resources.

The present study resolves these concerns, demonstrating accurate consensus-level SARS-CoV-2 sequence determination with ONT data. We report that: (*i*) SNVs at consensus-level read-count frequencies (80-100%) were detected with >99% sensitivity and >98% precision across 157 SARS-CoV-2-positive specimens, confirming the suitability of ONT sequencing for standard phylogenetic analyses; (*ii*) a minimum ~60-fold sequencing depth was required to ensure accurate detection of SNVs, but little or no improvement was achieved above this level; (*iii*) false-positive and false-negative variants were typically observed at low-complexity sequences, with fidelity improved by excluding these problematic sites; (*iv*) in contrast to consensus SNVs, ONT sequencing performed poorly in the detection of consensus indels or low-frequency variants (such variants should therefore be interpreted with caution); (*v*) while the high indel error rate in ONT sequencing impedes accurate detection of small indels, long nanopore reads appear well suited for the detection of large deletions and potentially other structural variants.

As the first systematic evaluation of nanopore sequencing for SARS-CoV-2 WGS, this study removes an important barrier to its widespread adoption in the ongoing COVID-19 pandemic. While short-read sequencing platforms remain the gold-standard for high-throughput viral sequencing, the advantages to portability, cost and turnaround-time afforded by nanopore sequencing imply that this emerging technology can serve an important complementary role in local, national and international COVID-19 response strategies.

MATERIALS & METHODS

Synthetic RNA controls

Synthetic controls used in this study were manufactured by Twist Biosciences and are commercially available (Catalog item 101024). The controls comprise synthetic RNA generated by *in vitro* transcription (IVT) of the SARS-CoV-2 genome sequence, representing the complete genome in 6 × ~5 kb continuous sequences. The controls used in this study are identical in sequence to the Wuhan-Hu-1 reference strain (MN908947.3), allowing sequencing artefacts to be readily identified. Synthetic controls were prepared for sequencing via a protocol established by the ARTIC network for viral surveillance (https://artic.network/ncov-2019). Briefly, reverse-transcription was performed on aliquots of synthetic RNA using Superscript IV (Thermo Fisher Scientific) with both random hexamers and oligo-dT primers. Prepared cDNA was then amplified using multiplexed PCR with 98 × ~400 bp amplicons tiling the SARS-CoV-2 genome (ARTIC V3 primer set). Amplification was performed with Q5 Hotstart DNA Polymerase (New England Biolabs) with 1.5 μL of cDNA per reaction. PCR products were cleaned using AMPure XP beads (0.8X bead ratio), quantified using a Qubit fluorometer (Thermo Fisher Scientific) and partitioned into separate aliquots for analysis by short-read and nanopore sequencing. We note that it is not possible to amplify the entire SARS-CoV-2 genome in this way, since amplicons that span boundaries of the 6 × ~5 kb IVT products necessarily fail. Nevertheless, we were able to evaluate ~95% of the SARS-CoV-2 genome sequence.

SARS-CoV-2 specimens

SARS-CoV-2-positive extracts from 157 cases, tested at NSW Health Pathology East Serology and Virology Division (SaViD), were retrieved from storage and included in this study. All specimens were nasopharyngeal swabs originating from patients in New South Wales during March-April 2020. Specimens underwent total nucleic acid extraction using the Roche MagNA Pure DNA and total NA kit on an automated extraction instrument (MagNA pure 96). Reverse-transcription was performed on viral RNA extracts using Superscript IV VILO Master Mix (Thermo Fisher), which contains both random hexamers and oligo-dT primers. Prepared cDNA was then amplified separately with each of 14 x ~2.5 kb amplicons tiling the SARS-CoV-2 genome, as described elsewhere[6]. Amplification was performed with Platinum SuperFi Green PCR Mastermix (Thermo Fisher) with 1.5 μL of cDNA per reaction. PCR products were cleaned using AMPure XP beads (0.8X bead ratio), quantified using PicoGreen dsDNA Assay (Thermo Fisher). All 14 x amplicon products from a given sample were then pooled at equal abundance and partitioned into separate aliquots for analysis by short-read and nanopore sequencing. This strategy ensured that any sequence artefacts potentially introduced during reverse-transcription and/or PCR amplification were common to matched ONT/Illumina samples, so would not be interpreted as false-positive/negatives during technology comparison.

Short-read sequencing

Pooled amplicons were prepped for short-read sequencing using the Illumina DNA Prep Kit, according to the manufacturer's protocol. Samples were multiplexed using Nextera DNA CD Indexes and sequenced on an Illumina MiSeq. The resulting reads were aligned to the Wuhan-Hu-1 reference genome (MN908947.3) using bwa mem (0.7.12-r1039)[30]. Primer sequences were trimmed from the termini of read alignments using *iVar* (1.0)[31]. Variants were identified using *samtools mpileup* (v1.9)[32] and filtered for a minimum quality of 20.

Nanopore sequencing

ARTIC amplicons (~400 bp) from the synthetic RNA controls were prepared for nanopore using the ONT Native Barcoding Expansion kit (EXP-NBD104). The longer amplicons (~2.5 kb) used on SARS-CoV-2 patient specimens were prepared for nanopore sequencing using the ONT Rapid Barcoding Kit (SQK-RBK004). Both kits were used according to the manufacturer's protocol. Up to twelve samples were multiplexed on a FLO-MIN106D or FLO-PRO002 flow-cell and sequenced on a GridION X5 or PromethION P24 device, respectively. The *RAMPART* software package[33] was used to monitor sequencing performance in real-time, with runs proceeding until a minimum ~200-fold coverage was achieved across all amplicons. At this point, the run was terminated and the flow-cell washed using the ONT Flow Cell Wash kit (EXP-WSH003), allowing re-use in subsequent runs.

The resulting reads were basecalled using *Guppy* (3.6) and aligned to the Wuhan-Hu-1 reference genome (MN908947.3) using *minimap2* (2.17-r941)[34]. The ARTIC tool *align_trim* was used to trim primer sequences from the termini of read alignments and cap sequencing depth at a maximum of 400-fold coverage. Consensus-level variant candidates were identified using *Medaka* (0.11.5). Sub-consensus level variant candidates were identified using *Varscan2* (v2.4.3)[35]. For further details see https://github.com/Psy-Fer/SARS-CoV-2_GTG.

Performance evaluation

For synthetic RNA controls, read-level quality metrics, such as sequencing error rates, were derived from read alignments using *pysamstats*, with any bases that differed from the Wuhan-Hu-1 reference sequence considered errors.

The accuracy of variant detection by ONT sequencing was evaluated by comparison to the set of variants identified by Illumina sequencing in matched cases. To ensure consistent representation of variants across calls generated by different programs: (*i*) multi-allelic variant candidates were separate into individual SNVs/indels using *bcftools norm* (1.9); (*ii*) multi-nucleotide variants were decomposed into their simplest set of individual components using *rtg-tools vcfdecompose* (3.10.1) and; (*iii*) indels at simple repeats were left-aligned using *gatk LeftAlignAndTrimVariants* (4.0.11.0). Variant candidates identified by Illumina/ONT could then be considered concordant based on matching genome position, reference base and alternative base/s. For a given case, variant candidates identified with ONT and Illumina were classified as true-positives (TPs), candidates identified by ONT but not Illumina as false-positives (FPs) and candidates identified by Illumina but not ONT as false-negatives (FNs). The following statistical definitions were used to evaluate results:

Sensitivity = TP / (TP + FN)

Precision = TP / (TP + FP)

Jaccard similarity = TP / (TP + FP + FN)

Structural variation

To identify structural variation, nanopore reads were re-aligned to the Wuhan-Hu-1 reference genome (MN908947.3) using the rearrangement-aware aligner *NGMLR* (v0.2.7)[36]. *Sniffles* (v1.0.11)[36] was then used to detect candidate variants with a minimum length of 10 bp and ≥ 20 supporting reads. To validate SVs detected with ONT alignments, split short-read alignments and discordant read-pairs were extracted from matched Illumina libraries using *lumpy*[37]. Variant candidates were then manually inspected to verify evidence from ONT and short-reads and assess break-point position resolution.

ACKNOWLEDGEMENTS

We acknowledge the following funding support: UNSW COVID-19 Rapid Response Research Initiative (to W.D.R.), MRFF Investigator Grant APP1173594, Cancer Institute NSW Early Career Fellowship 2018/ECF013 and philanthropic support from The Kinghorn Foundation (to I.W.D.).

AUTHOR CONTRIBUTIONS

Z.N., M.Y., K.W.K., S.S.B., W.D.R. & S.J.vH. oversaw collection and handling of SARS-CoV-2 specimens.

T.A., A.V. & I.S. performed cDNA synthesis and PCR amplification of SARS-CoV-2 samples.

J.M.H. & I.S. performed ONT library preparation and sequencing.

A.G.B. performed Illumina library preparation and sequencing.

J.M.F., H.G., I.S., S.J.vH. & I.W.D. performed bioinformatics analysis.

I.W.D. prepared the figures.

R.A.B., W.D.R., S.J.vH., & I.W.D. prepared the manuscript with support from co-authors.

DISCLAIMERS & COMPETING INTERESTS

J.F. & H.G. have previously received travel and accommodation expenses to attend ONT conferences. The authors declare no other competing financial interests.

REFERENCES

1. Wu, F. *et al.* A new coronavirus associated with human respiratory disease in China. *Nature* **579,** 265–269 (2020).
2. Zhu, N. *et al.* A Novel Coronavirus from Patients with Pneumonia in China, 2019. *N Engl J Med* **382,** 727–733 (2020).
3. Lu, R. *et al.* Genomic characterisation and epidemiology of 2019 novel coronavirus: implications for virus origins and receptor binding. *Lancet* **395,** 565–574 (2020).
4. van Kasteren, P. B. *et al.* Comparison of seven commercial RT-PCR diagnostic kits for COVID-19. *J Clin Virol* **128,** 104412 (2020).
5. Rambaut, A. *et al.* A dynamic nomenclature proposal for SARS-CoV-2 to assist genomic epidemiology. *bioRxiv* 2020.04.17.046086 (2020).
6. Eden, J.-S. *et al.* An emergent clade of SARS-CoV-2 linked to returned travellers from Iran. *Virus Evol* **6,** (2020).
7. Fauver, J. R. *et al.* Coast-to-Coast Spread of SARS-CoV-2 during the Early Epidemic in the United States. *Cell* **181,** 990–996.e5 (2020).
8. Gonzalez-Reiche, A. S. *et al.* Introductions and early spread of SARS-CoV-2 in the New York City area. *Science* eabc1917 (2020).
9. Gudbjartsson, D. F. *et al.* Spread of SARS-CoV-2 in the Icelandic Population. *N Engl J Med* NEJMoa2006100 (2020). doi:10.1056/NEJMoa2006100
10. Lu, J. *et al.* Genomic epidemiology of SARS-CoV-2 in Guangdong Province, China. *medRxiv* (2020). doi:10.1101/2020.04.01.20047076
11. Seemann, T. *et al.* Tracking the COVID-19 pandemic in Australia using genomics. *medRxiv* 2020.05.12.20099929 (2020).
12. Rockett, R. J. *et al.* Revealing COVID-19 Transmission by SARS-CoV-2 Genome Sequencing and Agent Based Modelling. *bioRxiv* 2020.04.19.048751 (2020).
13. Korber, B. *et al.* Tracking changes in SARS-CoV-2 Spike: evidence that D614G increases infectivity of the COVID-19 virus. *Cell* (2020).
14. Li, Q. *et al.* The impact of mutations in SARS-CoV-2 spike on viral infectivity and antigenicity. *Cell* (2020).
15. Uddin, M. *et al.* SARS-CoV-2/COVID-19: Viral Genomics, Epidemiology, Vaccines, and Therapeutic Interventions. *Viruses* **12,** (2020).
16. Jain, M., Olsen, H. E., Paten, B. & Akeson, M. The Oxford Nanopore MinION: delivery of nanopore sequencing to the genomics community. *Genome Biol.* **17,** 239 (2016).
17. Quick, J. *et al.* Rapid draft sequencing and real-time nanopore sequencing in a hospital outbreak of Salmonella. *Genome Biol.* **16,** 114 (2015).
18. Quick, J. *et al.* Real-time, portable genome sequencing for Ebola surveillance. *Nature* **530,** 228–232 (2016).
19. Quick, J. *et al.* Multiplex PCR method for MinION and Illumina sequencing of Zika and other virus genomes directly from clinical samples. *Nat Protoc* **12,** 1261–1276 (2017).
20. Rang, F. J., Kloosterman, W. P. & de Ridder, J. From squiggle to basepair: computational approaches for improving nanopore sequencing read accuracy. *Genome Biol.* **19,** 90 (2018).
21. Tyler, A. D. *et al.* Evaluation of Oxford Nanopore's MinION Sequencing Device for Microbial Whole Genome Sequencing Applications. *Sci Rep* **8,** 10931 (2018).
22. Laver, T. *et al.* Assessing the performance of the Oxford Nanopore Technologies MinION. *Biomol Detect Quantif* **3,** 1–8 (2015).
23. Rambaut, A. ***Phylodynamic Analysis | 176 genomes | 6 Mar 2020***. *virological.org* (2020).
24. Hardwick, S. A., Deveson, I. W. & Mercer, T. R. Reference standards for next-generation sequencing. *Nat. Rev. Genet.* **18,** 473–484 (2017).
25. Poirier, E. Z. & Vignuzzi, M. Virus population dynamics during infection. *Viral pathogenesis • Preventive and therapeutic vaccines* **23,** 82–87 (2017).
26. Worby, C. J., Lipsitch, M. & Hanage, W. P. Shared Genomic Variants: Identification of Transmission Routes Using Pathogen Deep-Sequence Data. *Am J Epidemiol* **186,** 1209–1216 (2017).
27. Gong, Y.-N. *et al.* SARS-CoV-2 genomic surveillance in Taiwan revealed novel ORF8-deletion mutant and clade possibly associated with infections in Middle East. *Emerging Microbes & Infections* **9,** 1457–1466 (2020).
28. Su, Y. C. *et al.* Discovery of a 382-nt deletion during the early evolution of SARS-CoV-2. *bioRxiv* 2020.03.11.987222 (2020).

29. Loose, M. W. The potential impact of nanopore sequencing on human genetics. *Hum Mol Genet* **26,** R202–R207 (2017).

30. Li, H. & Durbin, R. Fast and accurate short read alignment with Burrows–Wheeler transform. *Bioinformatics* **25,** 1754–1760 (2009).

31. Grubaugh, N. D. *et al.* An amplicon-based sequencing framework for accurately measuring intrahost virus diversity using PrimalSeq and iVar. *Genome Biol.* **20,** 8 (2019).

32. Li, H. A statistical framework for SNP calling, mutation discovery, association mapping and population genetical parameter estimation from sequencing data. *Bioinformatics* **27,** 2987–2993 (2011).

33. Mapleson, D., Drou, N. & Swarbreck, D. RAMPART: a workflow management system for de novo genome assembly. *Bioinformatics* **31,** 1824–1826 (2015).

34. Li, H. Minimap2: pairwise alignment for nucleotide sequences. *Bioinformatics* **34,** 3094–3100 (2018).

35. Koboldt, D. C. *et al.* VarScan 2: somatic mutation and copy number alteration discovery in cancer by exome sequencing. *Genome Res.* **22,** 568–576 (2012).

36. Sedlazeck, F. J. *et al.* Accurate detection of complex structural variations using single-molecule sequencing. *Nat. Methods* **15,** 461–468 (2018).

37. Layer, R. M., Chiang, C., Quinlan, A. R. & Hall, I. M. LUMPY: a probabilistic framework for structural variant discovery. *Genome Biol.* **15,** R84 (2014).

Table 1. Sequencing accuracy for Illumina and ONT whole-genome sequencing of synthetic SARS-CoV-2 controls.

Illumina samples	Reportable (bp)	Read-level error rate (errors per base per read)				Erroneous variants			Consensus accuracy
		Total	Mismatch	Deletion	Insertion	Total	SNVs	Indels	
A	28687	0.00152	0.00083	0.00058	0.00011	0	0	0	100%
B	28687	0.00153	0.00082	0.00060	0.00012	0	0	0	100%
C	28687	0.00148	0.00079	0.00057	0.00012	0	0	0	100%
D	28687	0.00172	0.00098	0.00063	0.00011	0	0	0	100%
E	28687	0.00124	0.00089	0.00024	0.00011	0	0	0	100%
F	28687	0.00170	0.00137	0.00023	0.00011	0	0	0	100%
G	28687	0.00122	0.00088	0.00022	0.00011	0	0	0	100%
H	28687	0.00118	0.00084	0.00024	0.00011	0	0	0	100%
Mean	28687	0.00145	0.00092	0.00041	0.00011	0	0	0	100%

ONT samples	Reportable (bp)	Read-level error rate (errors per base per read)				Erroneous variants			Consensus accuracy
		Total	Mismatch	Deletion	Insertion	Total	SNVs	Indels	
A	28192	0.06067	0.02093	0.02475	0.01499	0	0	0	100%
B	28192	0.06180	0.02150	0.02527	0.01503	0	0	0	100%
C	28192	0.06114	0.02141	0.02476	0.01496	0	0	0	100%
D	28192	0.06110	0.02146	0.02471	0.01493	0	0	0	100%
E	28192	0.06013	0.02067	0.02445	0.01501	0	0	0	100%
F	28192	0.05972	0.02018	0.02457	0.01496	2	0	2	99.9929%
G	28192	0.06178	0.02173	0.02486	0.01520	0	0	0	100%
H	28192	0.06030	0.02049	0.02470	0.01511	0	0	0	100%
Mean	28192	0.06083	0.02105	0.02476	0.01502	0.25	0	0.25	99.9991%

Table 2. Consensus-level accuracy of ONT whole-genome SARS-CoV-2 sequencing on patient specimens.
*Blacklist sites are error-prone low-complexity sequences (*n* = 15; 9-42 bp; see text for details).

	Global	Blacklist sites excluded*
Cases analysed	157	157
Genome coverage	99.59%	98.56%
Negative positions	4674554	4627768
Illumina SNVs	1194	1162
ONT SNVs	1209	1170
TPs	1188	1160
FNs	6	2
FPs	21	10
Sensitivity	99.50%	99.83%
Precision	98.26%	99.15%
Jaccard similarity	97.78%	98.98%
Perfect concordance	139/157 cases	144/157 cases
Illumina variants	1201	1162
ONT variants	1450	1323
TPs	1188	1160
FNs	13	2
FPs	213	118
Sensitivity	98.92%	99.83%
Precision	84.80%	90.77%
Jaccard similarity	84.02%	90.63%
Perfect concordance	50/157 cases	81/157 cases

Table 3. Detection of structural variation in SARS-CoV-2 specimens with ONT sequencing.

Specimen	SV type	Size	Gene	Supporting ONT reads	Short-read evidence	Breakpoint resolution
nCoV_077	Deletion	15	*orf1ab*	94	yes	0,0
nCoV_087	Deletion	88	*orf1ab*	48	no	.
nCoV_088	Deletion	34	*M*	75	yes	0,0
nCoV_106	Deletion	548	*orf1ab*	20	no	.
nCoV_125	Deletion	27	*ORF6*	20	yes	(-2,-3)
nCoV_183	Deletion	15	*ORF3*	41	yes	(-2,-2)
nCoV_214	Deletion	29	*S*	28	yes	(+1, +2)
nCoV_200	Deletion	328	*ORF8*	385	yes	yes
nCoV_209	Deletion	639	*orf1ab*	48	yes	yes
nCoV_211	Deletion	1840	*orf1ab*	22	no	.
nCoV_225	Deletion	328	*ORF8*	387	yes	yes
nCoV_235	Deletion	37	*M*	21	yes	(+3,+4)
nCoV_249	Deletion	702	*orf1ab*	52	yes	(-1,0)
nCoV_164	Deletion	588	*S*	59	yes	(+1, +4)
nCoV_083	Deletion	28	*S*	38	yes	yes
nCoV_083	Deletion	13	*N*	36	yes	(+1,+1)

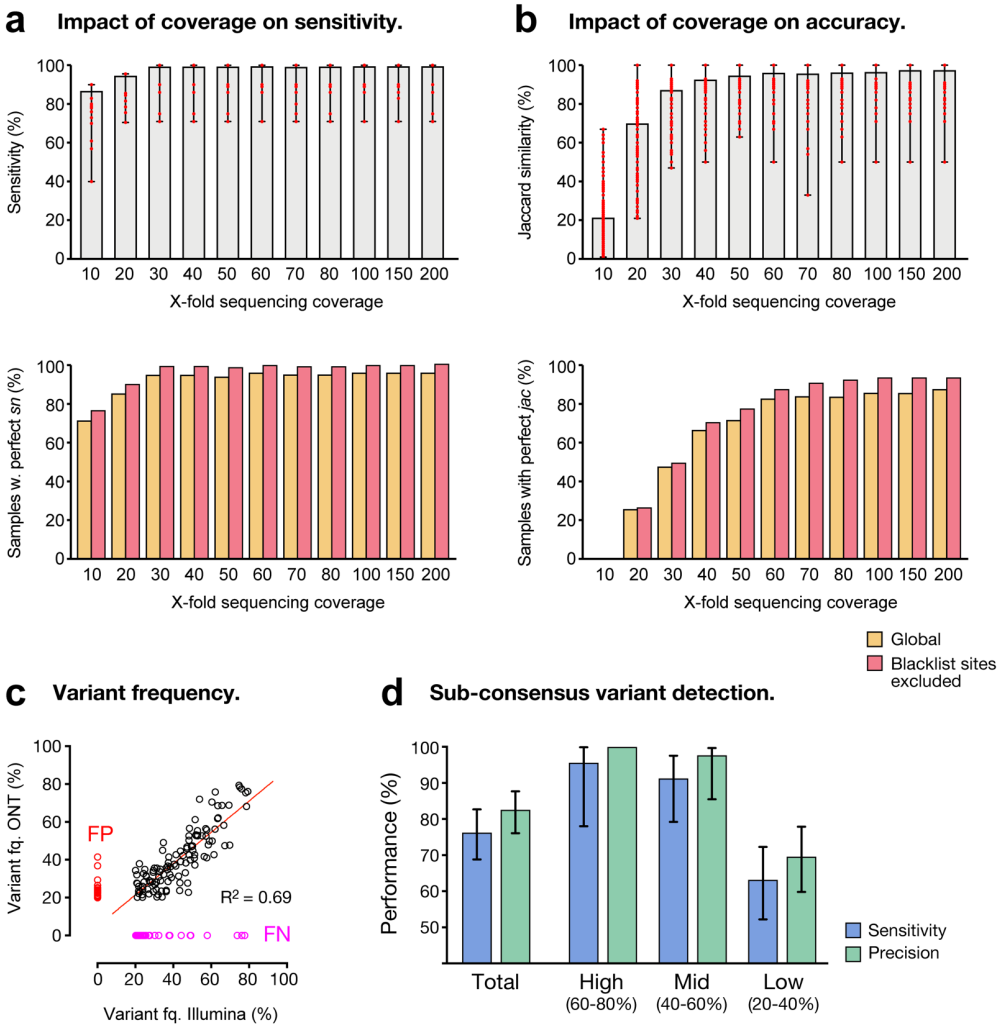

Fig. 1. Variant detection performance for whole-genome ONT sequencing of SARS-CoV-2. (**a**; upper) Sensitivity with which Illumina comparison SNVs at consensus-level variant frequencies (80-100%) were detected via ONT sequencing on matched SARS-CoV-2 specimens (*n* = 157). Bars show mean ± range. (**a**; lower) Fraction of specimens tested in which SNVs were detected with perfect sensitivity (*sn*). Data are plotted separately for genome-wide variant detection (gold) and variant detection with error-prone 'blacklist' sites excluded (red). (**b**) Same as in **a** but Jaccard similarity (*jac*) scores are plotted instead of *sn*. (**c**) Correlation of variant frequencies observed for SNV candidates detected at sub-consensus frequencies (20-80%) with Illumina and ONT sequencing. Candidates detected with ONT but not Illumina were considered to be false-positives (FP; red) and candidates detected with Illumina but not ONT were considered to be false-negatives (FP; pink). (**d**) Sensitivity (blue) and precision (green) of SNV detection with ONT sequencing at sub-consensus variant frequencies (20-80%). Data are plotted separately for high (60-80%), intermediate (40-60%) and low (20-40%) frequencies. Error bars show 95% confidence intervals (Clopper-Pearson).